Applied Catalysis A: General 455 (2013) 92–106

Contents lists available at SciVerse ScienceDirect

Applied Catalysis A: General

journal homepage: www.elsevier.com/locate/apcata

Transesterification of triacetin and castor oil with methanol catalyzed by supported polyaniline-sulfate. A role of polymer morphology

A. Drelinkiewicz[a,*], Z. Kalemba-Jaje[a], E. Lalik[a], A. Zięba[a], D. Mucha[a], E.N. Konyushenko[b], J. Stejskal[b]

[a] Institute of Catalysis and Surface Chemistry, Polish Academy of Sciences, Niezapominajek 8, 30-239 Kraków, Poland
[b] Institute of Macromolecular Chemistry, Academy of Sciences of the Czech Republic, Heyrovsky Sq. 2, 162 06 Prague 6, Czech Republic

ARTICLE INFO

Article history:
Received 27 August 2012
Received in revised form 18 January 2013
Accepted 22 January 2013
Available online 7 February 2013

Keywords:
Transesterification
Triacetin
Castor oil
Polyaniline

ABSTRACT

Polyaniline-sulfate deposited on three different carriers was studied for transesterification of triacetin and castor oil with methanol at mild reaction conditions (temperature of 55 °C). Multi-wall carbon nanotubes (CNT), carbon and silica were coated with polyaniline sulfate (ca. 20 wt%) during polymerization of aniline. Because of different textural and hydrophobic properties of the carriers, the polymer coatings of various morphologies were obtained as evidenced by the electron microscopy technique. A uniform coating of CNT with polymer resulted in the most extended polymer structure. Nanorods of polymer forming branched dendritic structures appeared in the other two carbon and silica carriers. The acid capacity and the strength of acid sites were similar in all studied catalysts. All the samples were found to be active solid acid catalysts in methanolysis of both studied triglycerides and CNT-coated polyaniline sulfate exhibited the highest activity. The course of reaction during methanolysis of triacetin on CNT-containing catalyst was similar to that in the presence of soluble sulfuric acid. On the other hand, a partial blockage of active sites was observed in carbon and silica coated with polyaniline sulfate. A blockage effect was ascribed to strong interaction of acid sites with more polar reagents among them diacetin and glycerol. These interactions were facilitated by aggregated fibriral morphology of the polymer coating resulting in locally high density of acid sites.

1. Introduction

Biodiesel fuel consisting of methyl esters of fatty acids is obtained in transesterification of triglycerides with methanol catalyzed by strong acids or bases. Owing to environmental, technological and economic reasons, the substitution of homogeneous catalysts by heterogeneous ones is a desirable goal. The advantage of solid catalysts consists of the ease of product separation and recycling of the catalyst. Recent studies concentrated mostly on solid acid catalysts as they are able to catalyze both transesterification of triglycerides and esterification of free fatty acids present in oil feedstock. A variety of solid acid catalysts has already been tested [1–5] and the sulfonic acid-based catalysts seem to be the most promising candidates. The examples include sulfate treated inorganic oxides such as zirconia, titania, tin oxide [6–10]. Another class of solid acid catalysts are organosulfonic groups-containing polymers such as Nafion, Amberlyst [5,11,12], various polystyrenes [13,14] as well as mesoporous silica materials [15–17]. Our previous work showed that polyaniline doped with sulfuric acid (Scheme 1) (PANI-S) was active and stable acid catalyst for the transesterification of triglycerides (triacetin and castor oil) and esterification of fatty acid (ricinoleic acid) with methanol [18,19]. Polyaniline salts such as hydrochloride, sulfate, nitrate were also reported by Palaniappan et al. [20–23] to be active catalysts for esterification of carboxylic acids (lauric, caprylic, acetic) and transesterification of ketoester (acetoacetate). Polyaniline sulphate was observed to be much more active than nitrate and hydrochloride salts [23]. Moreover, polyaniline sulfate showed almost fully stable activity evidenced by no essential change in the catalyst composition (leaching of sulphate) during the reactions [21–23].

The term "polyaniline" (PANI) refers to a polymer obtained by the oxidative polymerization of aniline. Due to nitrogen-containing groups, polyaniline exhibits basic character which allows easy doping of polymer with protonic acids to give the "polyaniline salt" (hydrochloride, sulfate etc.) [24]. Polyaniline salts are easy to prepare, handle, exhibit good environmental and thermal stability (temp up. to ca. 300 °C), are insoluble in most of organic solvents and they are organic semiconductors. These properties, and in particular electrical conductivity, make polyaniline salts a potential candidate to be used in optical and microelectronic devices, etc. From catalytic point of view, an interesting property of polyaniline sulfate is its high content of acid sites (4.75 mmol/g) [18,19] which

* Corresponding author. Tel.: +48 126395114; fax: +48 124251923.
E-mail address: ncdrelin@cyf-kr.edu.pl (A. Drelinkiewicz).

0926-860X/$ – see front matter © 2013 Elsevier B.V. All rights reserved.
http://dx.doi.org/10.1016/j.apcata.2013.01.022

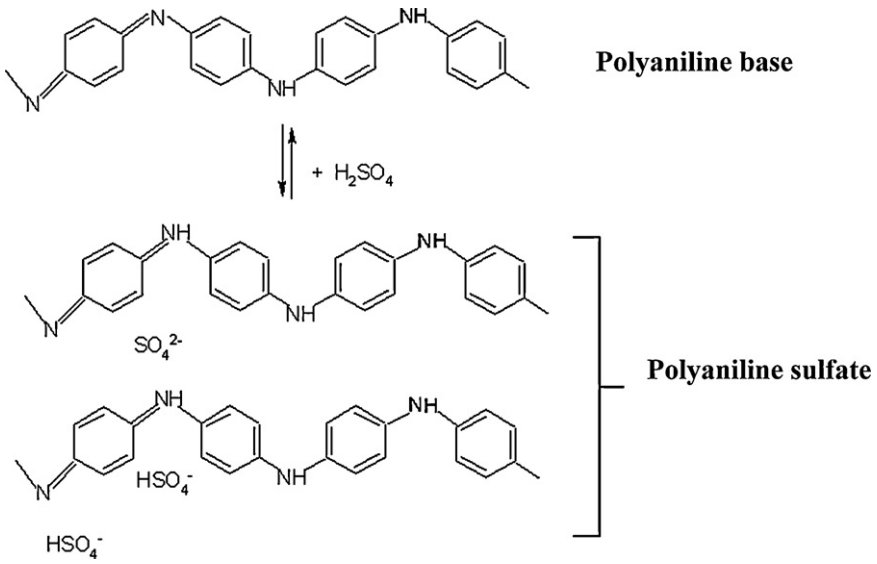

Scheme 1. The structure of polyaniline base and polyaniline sulfate.

is close to that of Amberlyst-15 commonly considered to be a catalyst of high acid capacity. On the other hand, PANI-sulfate exhibits relatively low specific surface area (25.9 m^2/g) [19] and does not swell in contact with reagents such as methanol, methyl esters or triglycerides. This results in not enough satisfactory utilization of active sites in the PANI-S powder catalyst.

However, strong adhering ability of polyaniline towards variety of materials (including glass, ceramics, inorganic oxides, metals, polymer microspheres, plastics, fibres, membranes) allowed deposition of polymer overlayer (submicroemter thickness) on the material surface [25]. The obtained polyaniline coatings exhibited an excellent resistance to solvent washing and manual scratching by sharp objects. Deposition of polyaniline salts was widely explored to modify electrical conductivity of the materials. Therefore these studies concentrated mostly on the role of polymerization conditions in electrical conductivity of polyaniline salts-coated samples. Polyaniline coatings could be produced by means of electrochemical as well as chemical procedures, among them by "in situ" adsorption polymerization of aniline performed in the presence of the materials. In this procedure the PANI-salts overlayer is formed by the immersion of the supporting material into an aqueous acidic solution of aniline containing an oxidant [26–30]. The coatings of polyaniline salts could exhibit various morphologies ranging from microspherical, rice-grain, coral-like cylinders, nanotubes and nanofibers. Nanofibers are often branched forming various networks, arrays and bundles.

The hydrophobous properties of the carrier surface were observed to play an important role in the process of polyaniline coating formation [26,31]. The coatings produced on hydrophobic surfaces like carbon were more uniform thus exhibiting more extended conformation. The tendency to develop the granular morphology of polyaniline was more pronounced for hydrophilic surfaces, such as glass, silica [31–36]. This was explained by a preferential adsorption of the reactive intermediates such as aniline cation radicals and oligomers onto the hydrophobic surface. This adsorption might change as a result of altered electron-density distribution caused by oligomers interactions with the surface of carriers.

From catalytic point of view, not only the morphology of polyaniline-coating but also the location of polymer throughout the particles of carrier seems to be important. However, to the best of our knowledge, no systematic studies were performed to examine a role of textural properties of carrier, like porosity, pore diameter, etc. These features could determine deposition of polymer more or less deeply inside the pore structure of the carrier. This could influence the access of active sites for the reactants and seems to be especially important in the case of relatively large triglyceride molecules, reactants in transesterification reaction.

Polyaniline sulfate-coated carbon samples were tested in our previous work [18]. Present studies are extended to other carriers, namely silica and multi-wall carbon nanotubes (CNT). The research is based on the polymerization of polyaniline sulfate in the presence of supports resulting in materials showing acid properties. The so-prepared catalysts have been thoroughly characterized by means of different experimental techniques including FTIR, XRD, nitrogen adsorption–desorption isotherms, ammonia sorption and microscopy (optical and SEM). Methanolysis is studied for triacetin (glycerol triacetate) (TACT) and castor oil. Reactivity of polyaniline sulfate-coated silica (SiO_2-PANI-S) and CNT (CNT-PANI-S) is compared with that of previously studied polyaniline sulfate-coated carbon (C-PANI-S) sample. The results obtained in the present work demonstrate that apart from textural properties (surface area, porosity) the support-sensitive morphology of polymer coating plays an essential role in catalytic reactivity of studied samples.

2. Experimental

2.1. Catalysts preparation

Polyaniline sulfate was deposited on carbon (Kemisorb, Kemira), silica (SP18 Kemira) and multi-wall carbon nanotubes (CNT). The physicochemical characteristics of CNT sample are described in previous papers [37,38]. Shortly, the multiwalled carbon nanotubes were manufactured by the firms L.MWNCTs-2040, Conyan Biochemical Technology, Taipei, Taiwan, diameter 40–80 nm in diameter, length 5–15 μm, and specific surface area 40–300 m^2/g [37].

Deposition of polymer was carried out in situ during the preparation of polyaniline by the method described earlier in detail [39]. The polymerization was performed by the oxidation of 0.1 M aniline sulfate with 0.25 ammonium peroxydisulfate in 50 vol.% ethanol–water at room temperature. Support was dispersed in ethanol, aniline sulfate was added and dissolved, followed by the equal volume aqueous solution of ammonium peroxydisulfate. A 100 cm^3 of this reaction mixture when used without support

generates approximately ~2 g of PANI-sulfate. If 8 g of silica is suspended in the reaction mixture at the beginning of reaction, polyaniline salt coats the surface of support with a thin submicrometre film. The content of polymer in the resulting composite material is thus ca. 20 wt%. The same applies to the coating of other supports, CNT and carbon material. General information on the principles of coating are described in a recent review article on this topic [26]. For ~20 wt% polymer loading, 200 cm^3 of reaction mixture was used per 20 g of support. Next day the coated support was separated, rinsed with 0.1 M sulfuric acid and acetone. The collected samples were dried at room temperature in air and then in desiccator over silica gel. Prior to catalytic test the samples were dried at temperature of 60 °C under reduced pressure.

Elemental analysis and thermogravimetric techniques were used to evaluate the content of PANI-sulfate in the obtained samples.

2.2. Characterization of catalysts

The specific surface areas of samples were calculated from the nitrogen adsorption–desorption isotherms at 77 K in an Autosorb-1, Quantachrome equipment. Prior to the measurements, the samples were preheated and degassed, under vacuum at 60 °C for 18 h. Pore size distribution was calculated using the BJH model based on nitrogen desorption isotherm. The FT-IR spectra were recorded using Bruker-Equinox 55 spectrometer and standard KBr pellets technique. Morphology of samples was studied by means of Field Emission Scanning Electron Microscope JEOL JSM – 7500 F. Elemental analysis was performed by means of CHNS-VarioEL III apparatus (Elementar Analysensysteme Hanau-Germany). The thermogravimetric measurements were performed using a NETZSCH STA 409 Luxx instrument within the temperature from 10 to 1000 °C (heating rate 30 °C/min) in an air atmosphere. Microscopic observations of catalysts before and after catalytic test were performed using inverted optical microscope (Nikon, Japan).

Microcalorimetric measurements of ammonia sorption were performed to determine the capacity and the strength of acid sites. Gas flow-through MICROSCAL microcalorimeter was used. The instrument measures the rate of heat evolution accompanying a solid–gas interaction. A sample is placed in a small microcalorimetric cell (7 mm in diameter) and the measurement is carried out in a flow-through mode. After thermally equilibrating the system, ammonia was adsorbed from the nitrogen carrier gas containing 3% of NH_3 flowing through the cell at 3 cm^3/min under normal pressure. Concurrently with the heat evolution, the uptake of ammonia from the carrier gas was measured by thermoconductivity detector (downstream detector, DSD). The completion of adsorption was signalled by cessation of the exothermic effect measured by microcalorimeter as well as by a plateau being reached in the downstream detector. At this point the pure nitrogen carrier was switched on and the endothermic effect of desorption was measured by calorimeter whereas the amount of the desorbed NH_3 was detected by DSD. The irreversible uptake of ammonia was calculated as a difference between the total uptake detected on the sorption and the release of ammonia observed on the subsequent desorption stage of the cycle. Similarly, the molar heats of the irreversible ammonia sorption were calculated as a difference of the total thermal effects of the sorption and desorption.

For selected samples, the capacity of acid sites was also determined by acid–base titration. The amount of ca. 0.1 g of each sample was suspended in 20 cm^3 of NaOH (0.1 M) for 24 h at room temperature. The liquid sample obtained after polymer filtration was subsequently titrated with 0.1 M HCl. The completeness of PANI-salt deprotonation after treatment by NaOH was checked by the FT-IR technique.

2.3. Catalytic tests

The transesterification of triacetin (Fluka) with methanol was carried out in a 100 cm^3 glass reactor at atmospheric pressure following the procedure reported in our previous publication [19]. Reactor was equipped with a reflux condenser, magnetic stirrer, and a tube for sampling the solution. In catalytic experiment, triacetin or castor oil, methanol and internal standard (toluene) were introduced to the reactor, heated up to a given temperature and then the catalyst was added.

The transesterification of triacetin (TACT) with methanol was typically performed at temperature of 55 °C using 2.6 cm^3 of triacetin and 16.2 cm^3 of methanol, i.e. at methanol to triacetin molar ratio (MR) of 29. The concentration of catalysts varied from 5.3 g/dm^3 to 15.8 g/dm^3, which corresponded to 0.33–1 wt% relative to the mass of triacetin. In the course of catalytic tests the samples of reaction mixture were periodically taken and analyzed by GC method following the method described earlier [19]. From the data of GC analysis the triacetin conversion (C_{TG}), and the yield of diacetin, monoacetin (Y_i) were calculated as follows:

$$C_{TG} = \frac{N_{TG,0} - N_{TG}}{N_{TG,0}} \times 100\% \quad (1)$$

$$Y_i = \frac{N_i}{N_{TG,0}} \times 100\% \quad (2)$$

where $N_{TG,0}$ and N_{TG} are the moles of triacetin initially present in the reactor and the moles of triacetin remaining at time t, respectively. N_i presents the number of moles of diacetin (N_{DI}) or monoacetin (N_{MONO}) in the reaction mixture at time t.

It was shown in our previous article that PANI-base powder did not exhibit activity for the methanolysis of triacetin. Furthermore, in the absence of catalyst only a trace conversion of triacetin (0.9% after 30 min of reaction) was observed [18,19].

The transesterification of castor oil with methanol was performed at 55 °C using 6 g of castor oil, 7.6 cm^3 of methanol (MR = 29) and 0.6 g of catalyst. This amount of catalyst corresponds to catalysts concentration in the reaction mixture equal to 43 g/dm^3.

Transesterification of castor oil at the same conditions as for triacetin (concentration of catalyst, 15.8 g/dm^3) resulted in very low yield of methyl esters. This is a consequence of definitively lower rate of reaction involving bulky triglycerides of castor oil. Therefore, in methanolysis of castor oil higher concentration of catalysts equal to 43 g/dm^3 was used. This concentration was chosen in our previous experiments [40].

The progress of reaction was monitored by GC analysis of methyl esters formed as described before [40]. Castor oil is entirely composed of a triglyceride of ricinoleic acid (87.44 wt%), traces of glycerol (below 0.1 wt%), di- and mono-glycerides of ricinoleic acid, and free ricinoleic acid (below 0.1 wt%). From the GC analysis of methyl esters apart from the dominating triglycerides of ricinoleic acid, low amounts of triglycerides of other fatty acids (linoleic 5.05 wt%, oleic 3.88 wt%, stearic 1.4 wt%, palmitic 1.28 wt%, linolenic 0.56 wt%, and other acids 0.39 wt%) were determined and the average molecular weight of castor oil was calculated to be 928 g/mol [40]. In discussion of catalytic results, the yield of methyl esters formed in methanolysis of castor oil was taken into consideration, identically to the method widely used in the case of vegetable oils.

As a measure of catalyst activity initial rate of methyl esters (ME) formation (below 10%) related to 1 g of catalyst was assumed [r (ME), mol ME/min g].

The catalytic tests were performed 2-times (in selected cases 3-times) and the average values are reported.

Esterification of ricinoleic acid with methanol was carried in the same reactor using 3 g of ricinoleic acid (Fluka) and 11.8 cm^3 of methanol (MR = 29) and 0.66 g of catalyst at temperature of 60 °C.

The progress of reaction was monitored by GC using the same analytical procedure as that in castor oil methanolysis.

3. Results and discussion

The supports used in the present work for deposition of polyaniline sulfate differ essentially in hydrophobic character and in textural properties (Table 1). Both carbon-based supports are more hydrophobic compared to silica support. The carbon support exhibits the highest surface area and the highest contribution of microporous structure. The other two CNT and SiO_2 supports are materials of lower specific surface area and mostly mesoporous structures.

In order to evaluate the content of polymer the catalysts were subjected to elemental analysis and thermogravimetric experiments. The data obtained by elemental analysis are not informative owing to high contribution of carbon originating from C and CNT supports. Furthermore, the content of sulfur determined by elemental analysis in all three samples is low (0.15–0.32 wt%) being close to the detection limit of the used technique. Previous investigations devoted to thermal behaviour of CNT coated with polyaniline sulphate [37] showed that thermal decomposition of polyaniline sulphate started at temperature of ca. 200 °C and was complete at 650 °C. The CNT material was thermally stable up to ca. 700 °C and become completely decomposed above 750 °C [37].

The content of polymer in the catalysts determined by thermogravimetric analysis as the loss of mass upon heating up to 600 °C is given in Table 2. This technique shows the content of polymer in the carbon supported C-PANI-S sample equal to 24.1 wt%. The content of ca. 20.2 wt% was determined in this sample as the increase of mass upon polyaniline deposition [18]. As shown in Table 2, the content of polyaniline sulphate in the catalysts ranges from 12.9 to 24.1 wt%.

The capacity of acid sites (mmol H^+/g of catalyst) is given in Table 2. Before discussing the acidity data some comment relative to the structure of polyaniline sulfate is needed. The catalysts were obtained by the polymerization of aniline in the presence of sulfuric acid. Recent results of Ayad et al. [41] demonstrated that two kinds of polyaniline sulfate may be formed (Scheme 1). At lower acidity of the medium, PANI-sulfate is formed by the association of one molecule of sulfuric acid per two imine nitrogen (structure 1), while at higher acidity two molecules of sulfuric acid may be introduced yielding PANI-hydrogen sulfate (structure 2). The values of H^+ capacity calculated assuming the formation of both polyaniline sulfate structures are summarized in Table 2. The capacities of protons in CNT-PANI-S and SiO_2-PANI-S catalysts (1.16 and 1.24 mmol H^+/g, respectively) are ca. two times higher than those of structure 1 but are close to those predicted by structure 2. Slightly higher value obtained for CNT supported sample may arise form the acid sites present in the CNT material.

The content of H^+ in carbon supported C-PANI-S sample (1.41 mmol H^+/g) although locates between that for structures 1 and 2, it seems to be nearest to the predicted value of structure 2. Thus, although both structures of polyaniline sulphate may appear, structure 2 corresponding to polyaniline hydrosulfate is the dominating one in the studied catalysts. However, for simplicity, all the catalysts are termed as "polyaniline-sulfate" – based samples.

In the present work FT-IR spectroscopy is used to confirm the presence of polyaniline sulfate in the catalysts. The spectra of catalysts and supporting materials are displayed in Fig. 1. Owing to relatively low content of polymer in the catalysts the bands originating from the polyaniline-sulfate are relatively weak. Nevertheless, spectral features originating from the protonated polyaniline can be recognized in the spectra of all studied catalysts.

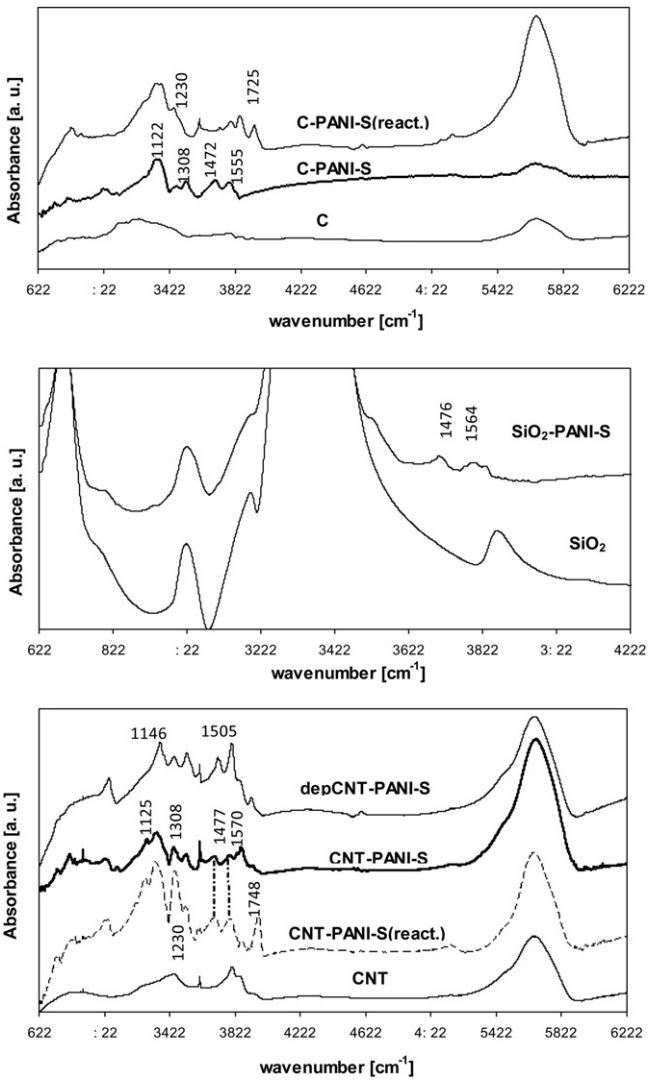

Fig. 1. FT-IR spectra of initial supports and polyaniline sulfate coated fresh and recovered catalysts.

The most characteristic bands of polyaniline are located at 1498 and 1589 cm^{-1}. They correspond to benzene and quinone ring-stretching deformations, the C—C in benzenoid and C=N and C=C bonds in quinonoid units, respectively [24]. Upon protonation of nitrogen groups and formation of polyaniline salts, the quinoid and benzenoid bands, both are shifted to lower wavenumbers, ca. 1479 and 1559 cm^{-1}. Other spectral feature originating from the vibrations of the doped segments of polyaniline chain is strong band at 1125 cm^{-1} and the peak at 1310 cm^{-1}, related to the C—N deformation mode. All these spectral features characteristic of PANI-salt (the bands located at 1555, 1472, 1308 and 1122 cm^{-1}) can be clearly recognized in the spectrum of carbon supported C-PANI-S catalyst. They are less distinct in silica-supported SiO_2-PANI-S catalyst because of strong overlapping bands originating from pure silica material. These are the peaks in the range of 1000–1300 cm^{-1} representing Si—O—Si stretching.

In the spectrum of CNT supported catalyst number of bands originating from CNT material appears. However, apart from them, two weak bands, characteristic of benzenoid and quinoid units of polyaniline-salt, located at 1477 and 1570 cm^{-1} appear. Moreover, strong band at 1125 cm^{-1} as well as the band at 1308 cm^{-1} due to protonated nitrogen groups can be easily recognized. For clarity, the spectrum registered for the deprotonated sample (treated by 0.1 M

Table 1
Physicochemical properties of catalysts.

Sample	Surface area [m^2/g]	Porosity [cm^3/g]	Pore diameter [nm]	Micro pore volume [cm^3/g]	Meso pore volume [cm^3/g]
Carbon (C)	734	0.39	1–2	0.199	0.191
C-PANI-S	347	0.13	1–2	0.037	0.093
Silica (SiO_2)	325	1.07	9.8	0.014	1.056
SiO_2-PANI-S	288	0.68	6.7	0.008	0.672
CNT	173	0.37	3.8	0.013	0.357
CNT-PANI-S	20	0.11	3.7	0	0.110

NH_3 (aq) for overnight) is also reported. It can be observed that in the spectrum of polyaniline base-containing sample, the bands of benzenoid units shifted to higher frequency, 1505 cm^{-1}, whereas the strong band at 1125 cm^{-1} vanished at the expense of the band at 1146 cm^{-1}, characteristic of polyaniline-base.

Thus, the FT-IR spectra of all studied catalysts exhibit the spectral features characteristic of PANI-salt. The band originating from the vibration of S-O groups is commonly observed at 1030–1050 cm^{-1}, i.e. at the position which is superimposed with the strong band at 1125 cm^{-1} arising from the protonated segments of polyaniline. This makes its observation difficult.

As described before, among all three supports carbon is material of the highest specific surface area and the highest contribution of microporous structure. The nitrogen adsorption–desorption isotherm of carbon support is typical for microporous materials (Fig. 2). Other two silica and CNT carriers exhibit lower specific surface area with lower contribution of micropores. The nitrogen adsorption–desorption isotherms and pore distribution diagrams show that both these supports are essentially mesoporous materials (Fig. 2). The isotherms for SiO_2 and CNT supports exhibit a hysteresis loop which is characteristic of mesoporous solids. The adsorption branch of isotherm for initial SiO_2 shows a sharp inflection. The sharpness of this step indicates relatively high uniformity of the mesopore size in the SiO_2 support which is calculated to be 9.8 nm. Deposition of PANI-S affects textural properties of all studied supports. This is manifested by the reduction of specific surface area and porosity of the supports. The contribution of both micropores and mesopores decrease due to the coating of the supports with polyaniline sulfate overlayer (Table 1).

However, the observed changes are different depending on the type of support material. This is evidenced by comparison of N_2 adsorption–desorption isotherms for initial and PANI-S-coated samples (Fig. 2). The changes in textural properties are the weakest in the case of silica support, i.e. material of less hydrophobous character. The reduction in specific surface area of silica particles is low (from 325 to 288 m^2/g) being the lowest among all studied supports. The N_2 adsorption–desorption isotherm of SiO_2-PANI-S sample (Fig. 2) exhibits a narrow hysteresis loop thus showing some changes in the porosity evidenced also by the pore distribution diagram.

The changes in surface area caused by deposition of polyaniline sulfate are considerably more distinct for carbon-based supports. The most dramatic changes can be observed for CNT support. Surface area and porosity of CNT material are dramatically reduced. In the polyaniline sulfate-coated CNT sample no microporous structure appears and its specific surface area (20 m^2/g) is dramatically lower than that of initial sample (173 m^2/g). The comparison of nitrogen adsorption–desorption isotherms for initial and PANI-S-coated CNT shows no essential change in their shape. As a result final CNT-PANI-S sample is mesoporous material of average pore diameter of 3.7 nm compared to 3.8 nm before polymer deposition. These changes in textural properties of CNT due to polyaniline deposition are consistent with the literature data [38].

Our previous results [19] demonstrated that surface area of carbon support decreased strongly from 734 to 347 m^2/g due to polyaniline sulphate deposition. As the data in Table 1 show this is accompanied by strong decrease in pore volume (from 0.39 to 0.13 cm^3/g) and in particular decreases the micropores volume. These results are consistent with the data reported by Avlyanov [42] who observed that surface area of carbon coated with ca. 20 wt% of PANI was about one half less than the surface area of initial carrier.

Data provided by the electron microscopy technique (SEM) demonstrate that the morphology of polyaniline sulfate coating is to high extent determined by the type of support (Figs. 3–6). The polymer nanorods agglomerated into interconnected networks forming branched fibrous structures can be seen for carbon and silica supported samples (Figs. 3 and 4). A more detailed inspection (images registered at high magnification ×50,000) reveals typical for polyaniline granular surface of nanorods in both catalysts. However, some differences in the shape, diameter, thickness and the extent of aggregation of nanofibiral structures in polymer coatings formed on silica and carbon materials exist. In carbon coated C-PANI-S catalyst, the nanorodes of polymer are relatively short and most of them are almost uniform in diameter 50–70 nm (Fig. 3). The nanorodes of polymer are remarkably thicker (90–100 nm in diameter) in the SiO_2-PANI-S catalyst and the branched dendritic structures are more aggregated (Fig. 4). Apart from these branched structures, a few rice-type polymer aggregates can be also observed. This shows a more compact morphology of PANI-S coating in silica-coated sample. The observed tendency to forming polymer coating of more compact morphology on the silica surface is consisted with the results of other authors [31,34] who observed that glass and silica surfaces produced polyaniline "island". This may suggest that PANI-S coating is deposited mostly onto outer most surfaces of silica particles and may explain definitively lower reduction in specific surface area and porosity of silica when compared with changes observed for carbon supports.

The morphology of polyaniline sulfate in CNT differs essentially from those in the carbon and silica – supported catalysts. The

Table 2
Acidic properties of studied catalysts.

Sample	PANI-S [wt%]	Heat of sorption kJ/mol NH_3	Calculated acid capacity mmol H^+/g catalyst		Measured acid capacity mmol H^+/g catalyst	
			Struct. I	Struct. II	Acid-base titration	NH_3 sorption
C-PANI-S	24.1	83.3	1.04	1.72	1.25	1.41
SiO_2-PANI-S	16.4	60.7	0.70	1.20	1.25	1.24
CNT-PANI-S	12.9	76.0	0.56	0.92	1.10	1.16

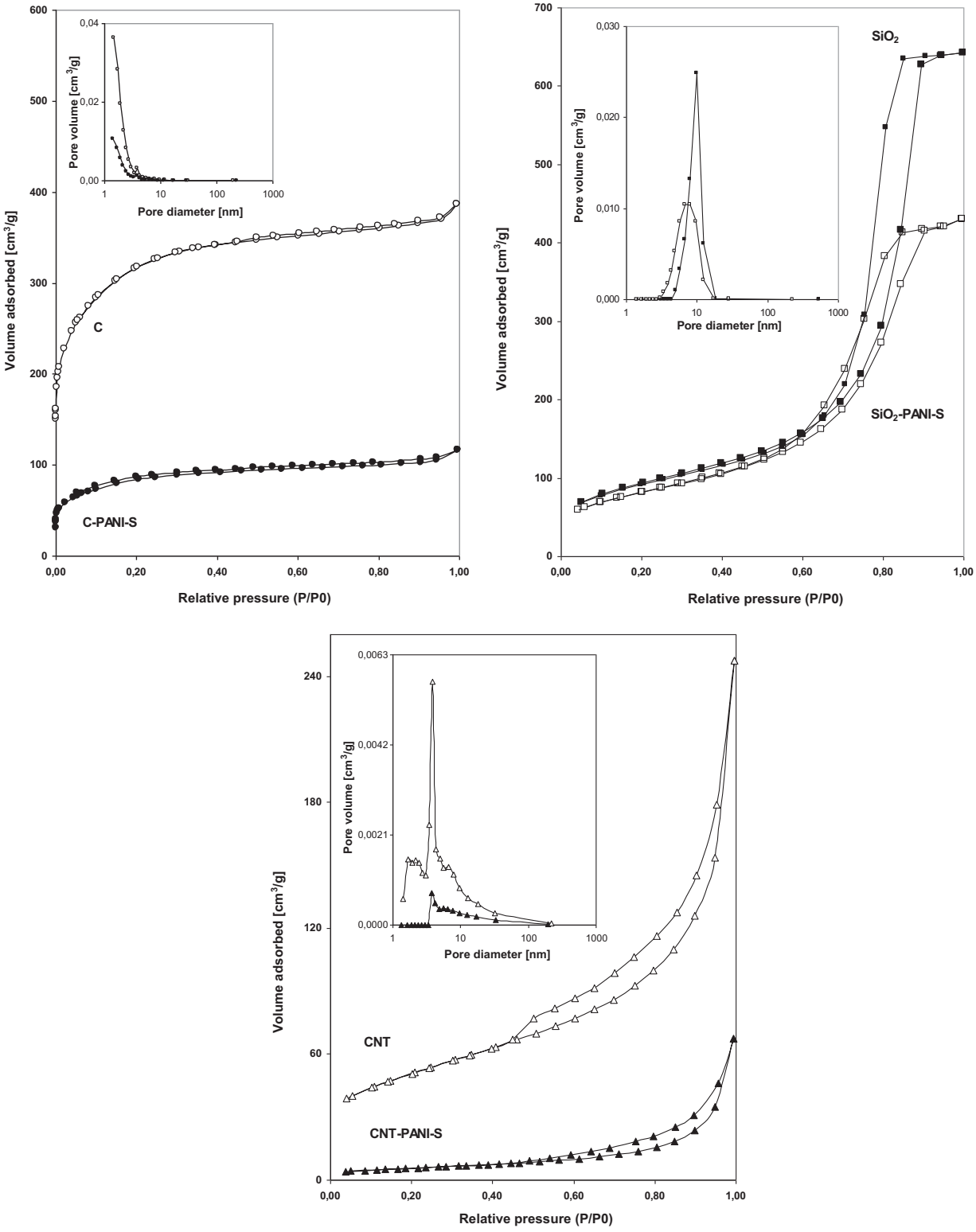

Fig. 2. Nitrogen adsorption – desorption isotherms and pore size distribution diagrams for initial supports and PANI-S coated samples.

micrographs presenting morphology of pristine and polyaniline sulfate coated CNT samples are displayed in Figs. 5 and 6, respectively. Previously reported data revealed that coating of CNT with polyaniline took place only at the outer surface of the CNT and the obtained coating was almost uniform [37,38]. In the obtained composite polyaniline localized exclusively at the surface of nanotubes created uniform layer capsulating individual particles of the supporting material and forming a structure labelled "fibre in a jacket" [37,38]. According to previous studies, the polymerization of aniline inside the CNT was hindered by the restricted access of reactants to the interior of the CNT [38]. This type of polyaniline overlayer is consisted with the literature data revelling the complete and uniform coating of CNT with various conductive polymers, among them polyaniline salts [43,44].

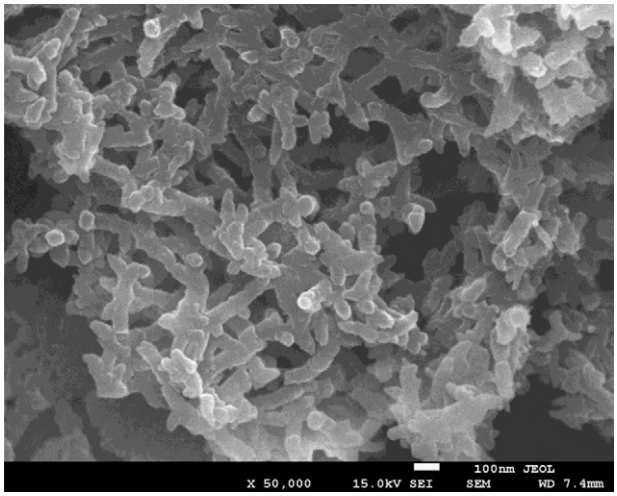

Fig. 3. SEM micrographs of C-PANI-S catalyst.

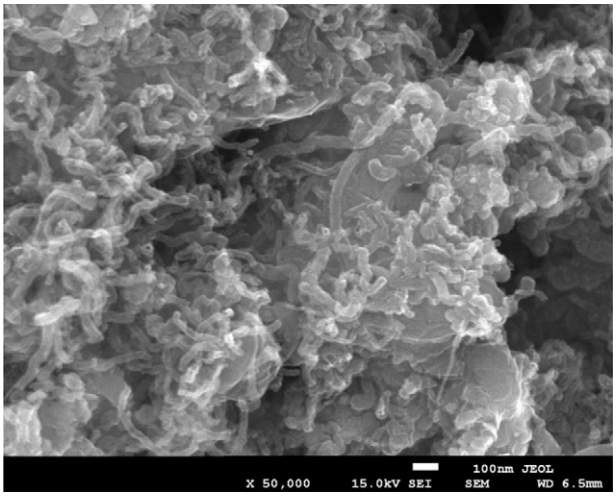

Fig. 5. SEM micrographs of initial CNT support.

The SEM micrographs (Fig. 5) show that initial CNT support consists of nanotubes 30–50 nm in diameter and their length is extended to several micrometres. The cavities in the nanotubes can be easily visible. Some nanotubes have no discernible cavity and could be rather regarded as nanorods. The PANI-S-coated material does not lose quasi-one-dimensional structure (Fig. 6). Polyaniline-coated CNT become thicker, 40–60 nm in diameter. Coating of CNT manifests by a more roughness surface of coated nanotubes whereas no fibrous network of polyaniline sulfate appears. Furthermore, no cavities in the nanotubes appear and some traces of polymer precipitate can be also observed. This demonstrates uniform coating of CNT with polymer leading to much extended polyaniline sulfate coating. This type of polymer coating may

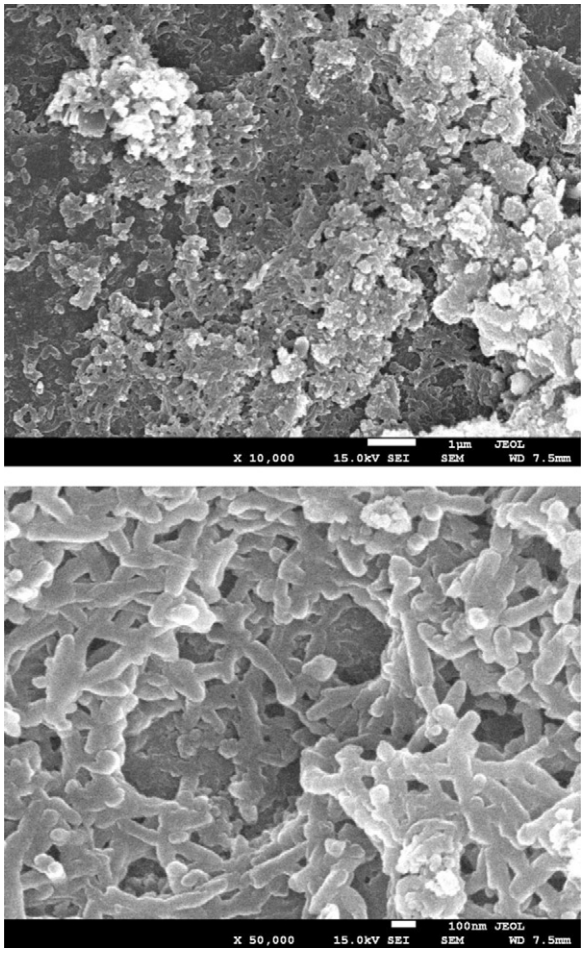

Fig. 4. SEM micrographs of SiO_2-PANI-S catalyst.

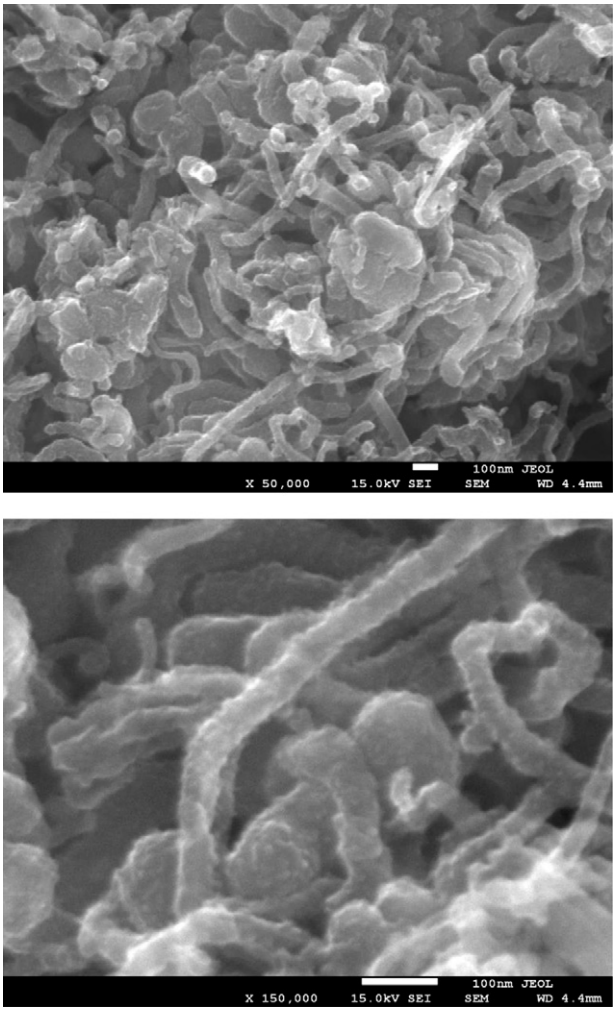

Fig. 6. SEM micrographs of CNT-PANI-S catalyst.

explain strong reduction of CNT surface area and porosity due to the polymer deposit.

Thus, textural and hydrophobous features of support material influence the process of polyaniline sulfate deposition. More hydrophobous carbon-based supports produce better extended overlayers of polyaniline sulfate than that formed on less hydrophobous silica material. This is evidenced by more dramatic reduction of specific surface area and porosity of both carbon-based supports compared to that for silica carrier. The most extended polymer coating is formed on CNT support.

The acid capacity (mmol H^+/g of catalyst) was determined using ammonia sorption technique. For selected catalysts the acid–base titration method was also involved to determine the acid centres content. The obtained data are collected in Table 2. From the sorption experiments the heat of ammonia sorption (kJ/mol NH_3) was also determined. This value is assumed to be a measure of the strength of acid centres in the samples. As shown in Table 2, studied catalysts exhibit similar acid characteristics. The content of H^+ ranges from 1.16 to 1.41 mmol/g. The heat of ammonia sorption is within similar range, 60.7–83.3 kJ/mol. However, the heat obtained for SiO_2-PANI-S catalyst (60.7 kJ/mol) is slightly lower when compared with both carbon-based samples. This may suggest that interactions of structural units of polyaniline with silica surface are somewhat different than interactions with carbon materials.

3.1. Catalytic experiments

As described before, PANI-sulfate-based catalysts were studied in our previous works [18,19]. The PANI-sulfate powder catalyst and carbon supported catalysts with various loading of polyaniline-sulfate (13–26 wt%) were tested. It was established that the PANI-S powder as well as PANI-S-coated carbon samples could be used repeatedly without essential loss in catalytic activity. In the present work catalytic properties of PANI-S-coated CNT and silica are compared with that of previously studied C-PANI-S catalyst with capacity of acid sites 1.41 mmol H^+/g. Here, methanolysis experiments are carried out at the same conditions as those in previous experiments. The methanol to triacetin molar ratio of 29:1 is used.

In order to evaluate any possible contribution of some PANI-S soluble in methanol in the catalytic performance, the catalysts were stirred for 3 h at 55 °C under methanol reflux. Then, methanol obtained after filtration was used in methanolysis of triacetin. The triacetin conversion of ca. 1% was observed after 30 min of reaction. Our previous results showed a trace conversion of triacetin (ca. 0.9% after 30 min of reaction) in blank catalytic experiment carried out in the absence of catalyst [18,40]. Moreover, similarly to previously used procedure, the obtained methanol filtrate was also analyzed for the presence of sulfate ions using a sensitive analytical test with Ba^{2+} ions. After addition of $BaCl_2$ solution no precipitate was observed. It seems therefore that no free sulfuric acid appears in the catalysts.

The activity of PANI-S coated catalysts is also compared with that of previously studied PANI-S powder and Amberlyst-15 catalysts. As a measure of catalyst activity, initial rate of triacetin conversion (below 10% conversion) calculated per mass of catalyst is assumed. The initial rates calculated per unit mass of catalyst are collected in Table 3. As described before, the capacity of acid sites in the PANI-S powder and in Amberlyst-15 are similar 4.75 and 4.70 mmol H^+/g, respectively. The initial rate of triacetin conversion in the presence of Amberlyst-15 (2.26×10^{-4} mol min^{-1} g^{-1}) was determined to be only slightly higher than the rate on PANI-S (1.76×10^{-4} mol min^{-1} g^{-1}) powder catalysts [19]. The same relation was obtained in methanolysis of castor oil. The initial rate of methyl ester (ME) formation on Amberlyst-15 was determined to be 0.125×10^{-4} [mol (ME) min^{-1} g^{-1} (cat)]. A similar rate equal to

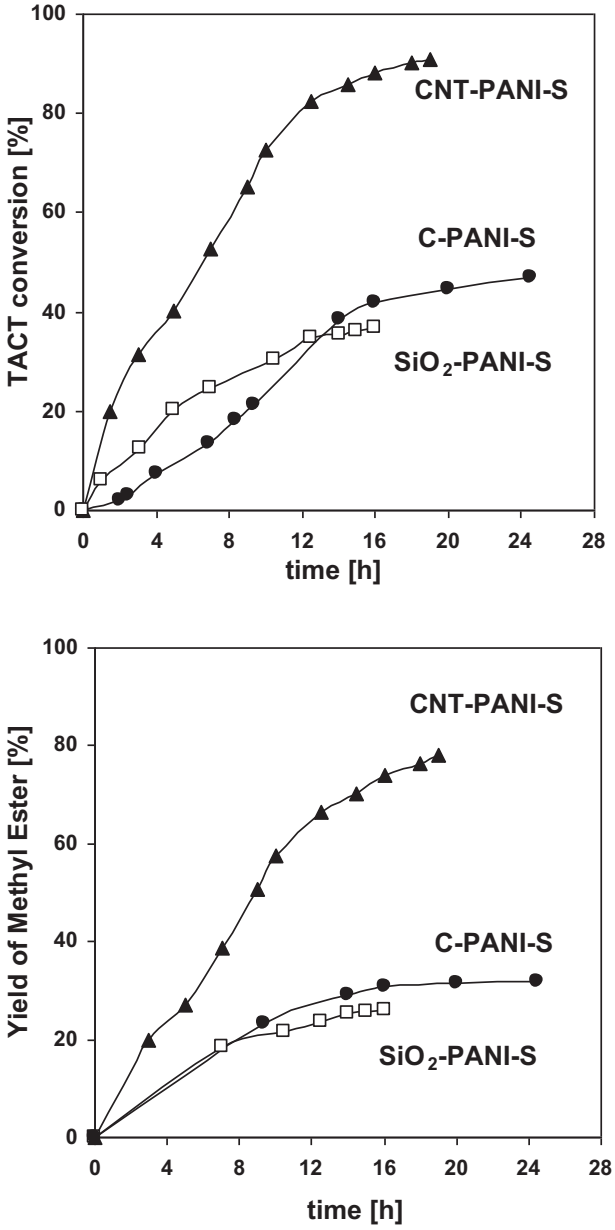

Fig. 7. The conversion of TACT and the yield of methyl ester against reaction time. Reaction conditions: catalyst concentration 15.8 g/dm^3, temperature of 55 °C, methanol: TACT = 29:1 molar ratio.

0.120×10^{-4} [mol (ME) min^{-1} g^{-1} (cat)] was obtained on PANI-S powder catalyst.

The time conversion plots for the methanolysis of triacetin on PANI-S coated catalysts demonstrate that all studied catalysts are active in the reaction (Fig. 7). The most active is CNT-PANI-S catalyst whereas the activity of other two catalysts is lower and PANI-S-coated carbon exhibits the lowest activity. The same relation is preserved when the yield of methyl esters is taken into consideration (Fig. 7). The comparison of initial activities related to mass of catalyst [expressed as mol TACT min^{-1} g^{-1} (catalyst)] (Table 3) clearly demonstrates that CNT-supported catalyst is ca. 5-times more active than the less active carbon-supported sample.

Fig. 8 shows the comparison of triacetin methanolysis in the presence of the most active CNT-PANI-S catalyst and in homogeneous reaction catalyzed by dissolved sulfuric acid. According to the literature and our previous results [18] from the very beginning of homogeneous reaction catalyzed by sulfuric acid both partial

Table 3
Activity data obtained in methanolysis of triacetin and castor oil.

Catalyst	TACT methanolysis[b]			Castor oil methanolysis[c]
	Conversion (3 h) [%]	Initial rate [mol TACT min^{-1} g^{-1} (cat)] $\times 10^{-4}$	Initial rate [mol TACT min^{-1} mol^{-1} H^+] $\times 10^{-2}$	Initial rate [mol (ME) min^{-1} g^{-1} (cat)] $\times 10^{-4}$
Amberlyst-15	50.2	2.26	4.80	0.125
PANI-S powder	42.8	1.76	3.70	0.120
C-PANI-S	4.7	0.14	1.00	0.011
	4.4[a]	0.13[a]	0.98[a]	
SiO_2-PANI-S	15.5	0.42	3.36	0.009
	13.9[a]	0.38[a]	3.26[a]	
CNT-PANI-S	31.4	0.78	6.70	0.048
	28.7[a]	0.62[a]	6.30[a]	

[a] Data obtained in recycling use of the catalysts. The samples were treated with methanol/THF mixture.
[b] Reaction conditions: temperature 55 °C, catalyst concentration 15.8 g/dm^3, methanol:TACT = 29:1.
[c] Reaction conditions: temperature 55 °C, catalyst concentration 43 g/dm^3, methanol:TACT = 29:1.

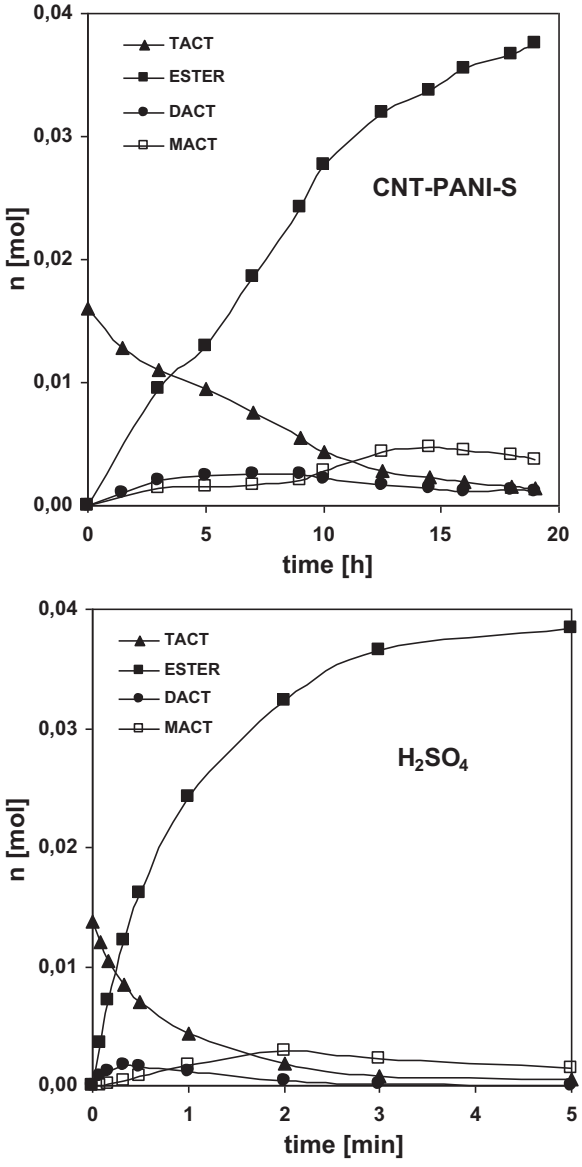

Fig. 8. Reagents distribution in methanolysis of triacetin catalyzed by CNT-PANI-S and soluble H_2SO_4. Methanolysis of TACT on CNT-PANI-S: catalyst concentration 15.8 g/dm^3, temperature of 55 °C, methanol: TACT = 29:1 molar ratio. Reaction catalyzed by soluble sulfuric acid: H_2SO_4 concentration $1{,}62 \times 10^{-2}$ mol/dm^3, temperature of 55 °C, methanol: TACT = 29:1 molar ratio.

glycerides diacetin and monoacetin are formed and their contents pass through the maximum. The maximum yield of diacetin corresponds to 13.6% and is attained at ca. 45% triacetin conversion. The maximum yield of monoacetin is observed at higher triacetin conversion, ca. 90%. In final solution, the triacetin conversion higher than 95% could be attained. As Fig. 8 shows the course of consecutive reactions on CNT-PANI-S catalyst is similar to that under homogeneous conditions. The maximum yield of diacetin (15.6%) formed on CNT-PANI-S is only slightly higher than that in homogeneous reaction (13.6%). The difference between these two catalysts is more pronounced relative to the monoacetin. The amount of monoacetin formed on CNT-PANI-S catalyst is higher than that under homogeneous conditions.

However, the course of consecutive reactions during methanolysis of triacetin on CNT-PANI-S catalyst differs essentially from those on other two C-PANI-S and SiO_2-PANI-S catalysts. This is evidenced by the conversion plots in Fig. 7. In the presence of CNT-PANI-S catalyst the maximum triacetin conversion attains 91%. On the other hand, in the presence of other two catalysts, after consumption of ca. 30–40% of triacetin, the rate of its further conversion starts to slow down remarkably. This effect suggests a blockage of active sites in these two catalysts. To better recognize this effect it is interesting to follow the formation of partial glycerides, diacetin and monoacetin. As shown in Fig. 9 the change in their content is strongly dependent on the type of catalyst. The yields of both partial glycerides diacetin and monoacetin are the lowest on CNT-PANI-S catalyst and as shown in Fig. 8 they pass through the maxima. The contents of both partial glycerides are remarkably higher on C-PANI-S and SiO_2-PANI-S catalysts. Within the whole triacetin conversion the yield of diacetin is the highest on microporous carbon-supported C-PANI-S catalyst. At 40% TACT conversion a distinct plateau corresponding to diacetin yield of ca. 30% is reached and after that the content of diacetin practically does not decrease. The effect of plateau shows that although diacetin is formed, it is not further reacted to monoacetin as well as the reverse transformation of diacetin to triacetin is strongly inhibited. This demonstrates almost complete blockage of the active sites in the C-PANI-S catalyst. As a result, the yield of methyl ester is definitively lower than that predicted from the obtained conversion of triacetin. This is evidenced by the graph showing the yield of methyl ester (Fig. 8).

On SiO_2-PANI-S catalyst the yield of diacetin is lower than that on C-PANI-S (Fig. 9) thus suggesting that although a blockage of active sites appears, it is definitively weaker.

The reaching of plateau by diglyceride has been observed by Cantrell et al. [45] in methanolysis over alkaline solid catalysts, Mg–Al hydrotalcites as well as CaO and MgO catalysts [46]. This effect was ascribed to a detrimental role of glycerol/partial glycerides interactions with the active sites of alkaline catalysts which resulted in the creation of glycerol/glycerides film onto the solid

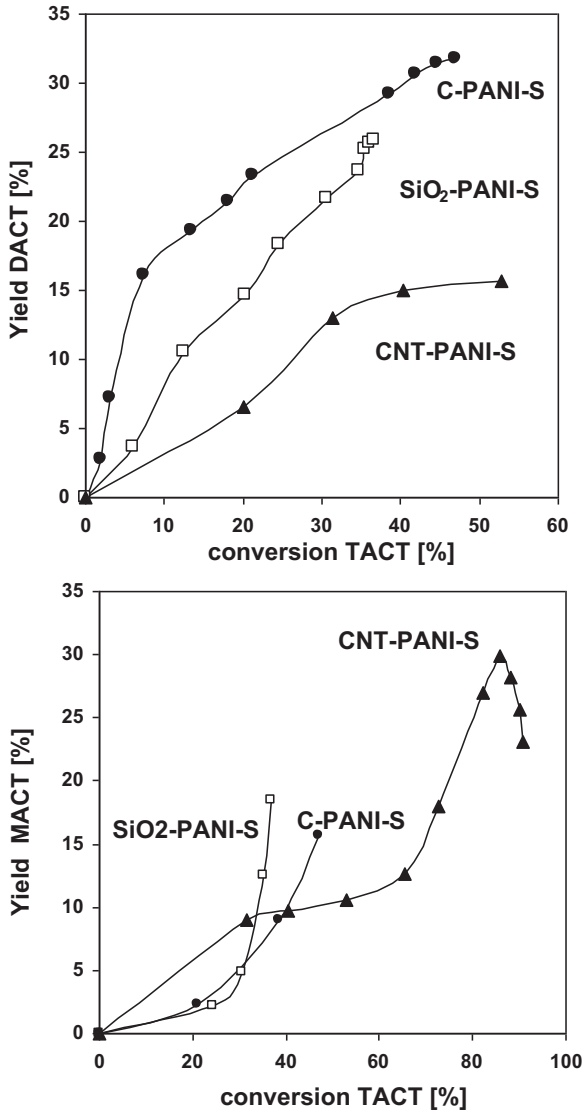

Fig. 9. The yield of diacetin (Y_{DI}) and monoacetin (Y_{MONO}) in methanolysis catalyzed by CNT-PANI-S, C-PANI-S and SiO_2-PANI-S samples. Reaction conditions: catalyst concentration 15.8 g/dm^3, temperature of 55 °C, methanol: TACT = 29:1 molar ratio.

catalyst. The presence of this glycerol/glycerides film could be a mass transfer barrier to the methanol and triglycerides as well as it could facilitate the reverse reactions [46]. On the other hand, esterification of glycerol with fatty acids to form monoglycerides catalyzed by acid sites in Amberlyst resin was significantly inhibited due to strong interaction of glycerol with the active sites. This was result of specific solvation properties of polyols (glycerol) leading to the formation of system of hydrogen bonds with the participation of glycerol OH-groups and the acid groups of catalyst [47].

Thus, in view of literature reports, the observed effect of "plateau" reaching by diacetin may be ascribed to the accumulation of glycerol/partial glycerides on the catalyst surface. This can be result of strong interactions of more polar reagents with acid sites of polyaniline-sulfate. However, textural properties of catalyst like porosity as well as polymer morphology may also contribute to the blockage effect. These effects are discussed in the next paragraph.

The effect of catalyst concentration is studied using CNT-PANI-S and C-PANI-S samples (Fig. 10). In experiments, the amount of catalyst was varied keeping other parameters constant. The TACT conversion obtained after reaction time of 3 h is taken into consideration as a measure of reaction rate. When the content of both catalysts increases the transesterification occurs at a faster rate. The reaction rate increases almost proportionally with the growth in the concentration of the CNT-PANI-S catalyst within the range employed in the studies (Fig. 10). According to Pappu et al. [48] who studied kinetic model for triglyceride transesterification on Amberlyst-15, the linear plot shows that the catalyst is effectively distributed and active throughout the reaction mixture. On the other hand, although the TACT methanolysis is faster as the concentration of C-PANI-S catalyst increases, there is no proportional growth.

Fig. 11 demonstrates the influence of reaction temperature on the conversion of triacetin. The data obtained in the presence of CNT-PANI-S catalyst are compared with those on C-PANI-S catalyst. When the temperature increases from 35 to 55 °C the rate of TACT conversion remarkably grows on CNT-PANI-S catalyst. On the other hand, the temperature of reaction has definitively weaker effect in the case of C-PANI-S catalyst. From the initial rates of TACT transesterification (below 15% conversion) the activation energy is determined using Arrhenius plots reported in Fig. 11. For both studied catalysts, the linear relationships are obtained within the temperature range employed in experiments. By linear regression analysis, the apparent activation energy is evaluated to be 54.5 kJ/mol for TACT conversion on CNT-PANI-S catalyst. Definitively lower value of activation energy, 14.3 kJ/mol is calculated for C-PANI-S catalyst. The activation energy obtained on CNT-PANI-S catalyst is close to the data obtained on powder PANI-S (50.5 kJ/mol [19]) as well as to those reported by other authors for methanolysis catalyzed by acid catalysts. For triacetin methanolysis on Nafion SAC-13 composite activation energy of 48.5 kJ/mol was reported, which was comparable to that for triglycerides methanolysis catalyzed by soluble acids (*p*-toluenesulfonic 50.7 kJ/mol, sulfuric 46.1 kJ/mol) [12,49]. Thus, apparent activation energy for TACT methanolysis obtained on CNT-PANI-S catalyst is within the range predicted by the other authors for reaction under mass-transfer free conditions.

The effects observed for C-PANI-S catalyst namely very weak influence of concentration of catalyst and reaction temperature may suggest diffusion limitation. During transesterification of natural oils mass-transfer limitations may occur because the reaction system contains a methanol phase, an oil phase and a solid-catalyst phase. With the increase of methyl esters yield, biodiesel can change the phase equilibrium and promote the mutual dissolving of oils and methanol. When the produced biodiesel makes methanol dissolve all oils completely, the system becomes a liquid–solid reaction. Therefore, the reaction system contains a heterogeneous liquid–liquid–solid reaction stage and a liquid–solid reaction stage. However, reports on kinetics studies have focused mostly on homogeneous catalysts. Recently published few papers focusing on kinetics on solid base as the catalyst demonstrated that methanolysis of soybean oil on CaO, SrO was controlled by both mass-transfer and reaction. However, the mass transfer resistance was higher than the reaction resistance. The authors concluded that the main mass transfer resistance lay on the surface of the catalyst particles [50]. Mass-transfer limitations resulting due to microporous structure of Dowex-type resin were also observed to be crucial for methanolysis of coconut oil [51].

In the present reaction mixture no phase separation exists, because all reagents, triacetin, methanol and methyl esters are well miscible. However, liquid–solid mass-transfer limitation may be encountered and as described before, accumulation of glycerol/partial glycerides on the active sites may be a barrier for the transport of reactants to/from the active sites.

In order to follow catalysts blockage effect the recovered catalysts are subjected to FT-IR and optical microscopy experiments. The samples of catalysts were taken from the reaction mixture

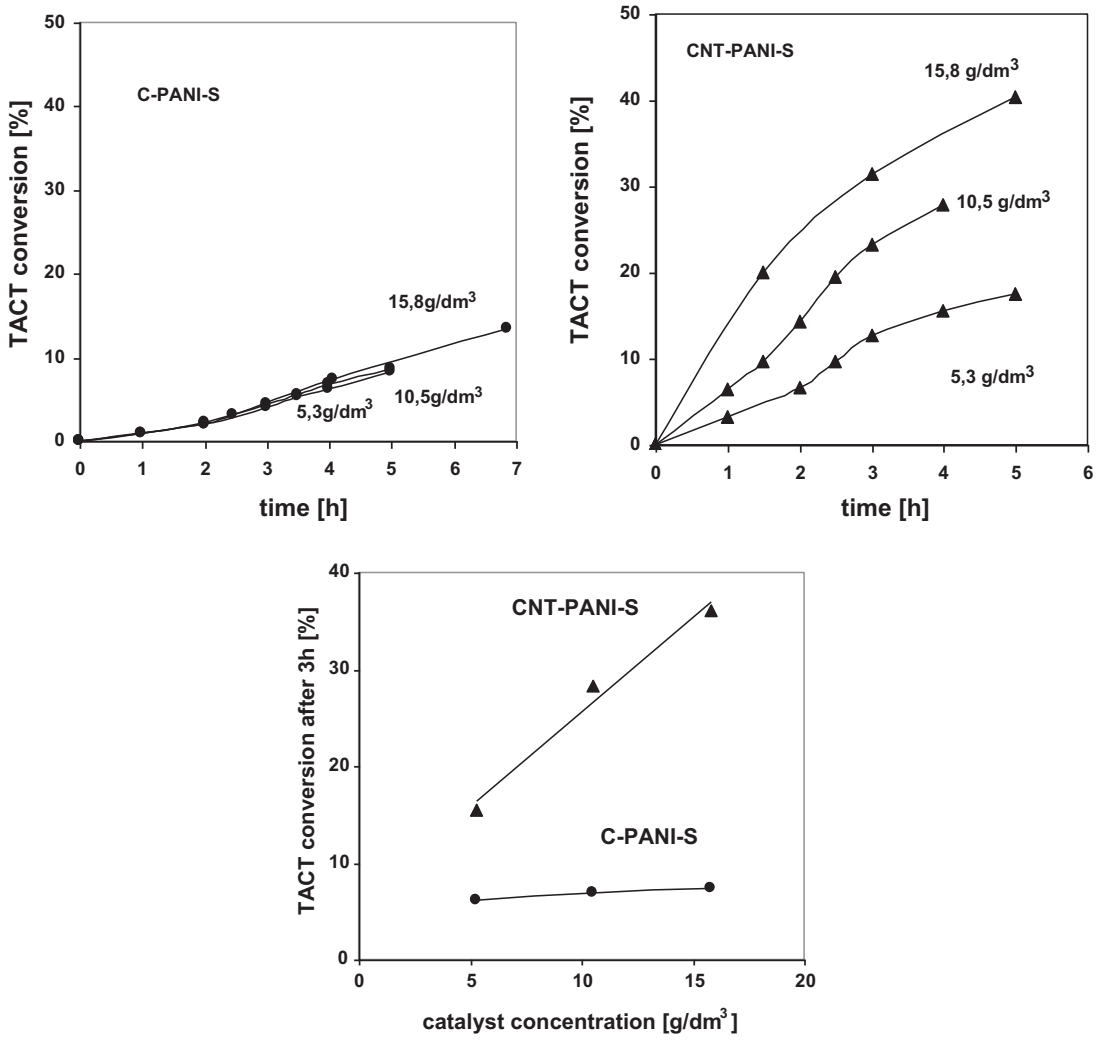

Fig. 10. The effect of CNT-PANI-S and C-PANI-S catalysts concentration. Reaction conditions: temperature of 55 °C, methanol: TACT = 29:1 molar ratio.

(after 10 h of reaction) and allowed to stay in air up to dryness. The FTIR spectra of fresh and recovered (not washed catalysts) are displayed in Fig. 1. For the comparison, the spectra of triacetin, diacetin and glycerol are also reported (Fig. 12). A similar set of bands characteristic of C—O in ester groups can be observed in the spectra of both glycerides. They are located at frequency of 1040, 1369 and 1740 cm^{-1}. However, the position of the most intense band differs in the frequency. This band is observed at 1212 cm^{-1} in the triacetin spectrum and at higher frequency, i.e. 1230 cm^{-1} in the spectrum of diacetin. Moreover, in the spectrum of diacetin a broad band at ca. 3400 cm^{-1} originating from the hydrogen bonds can be observed. In the FT-IR spectrum of glycerol apart from a strong and broad peak arising from the hydrogen bonds (at ca. 3400 cm^{-1}) also an intense band at 1040 cm^{-1} together with a not well resolved bands within the range 1400–1600 cm^{-1} appear.

In the spectrum of recovered C-PANI-S catalyst apart from the bands originating from the catalyst also a few new bands arising from the glycerides/glycerol can be observed. Well observable are the bands at 1725, 1380 and 1240 cm^{-1} as well as a strong band at 3400 cm^{-1} characteristic of hydrogen bonds. Their presence and in particular the one at 1240 and 3400 cm^{-1} can be ascribed to diacetin. However, it cannot be excluded from these spectral features that apart from diacetin, glycerol also appears in the recovered C-PANI-S catalyst. Similar spectral effects can be observed for recovered CNT-PANI-S catalyst. In the spectrum of this catalyst apart from a number of bands originating from the polyaniline and CNT support also the band at 1748 cm^{-1} arising from the glycerides appears. However, similarly to the previous spectrum for C-PANI-S catalyst the band at 1230 cm^{-1} characteristic of diacetin can be also recognized. It should be pointed out that in the spectrum of recovered CNT-PANI-S catalyst the position of the bands characteristic of protonated polyaniline does not change relative those in the spectrum of initial catalyst. This indicates that polymer is still in the protonated form and the acid sites are not removed during the catalytic tests. It should be pointed out that spectral observations for SiO_2-PANI-S catalyst are practically impossible owing to a presence of strong band originating form silica material.

The microscopic images registered for initial and recovered catalysts are displayed in Fig. 13. The optical microscopy was used because this technique allows observing the samples without special treatment procedure like vacuum treatment during the SEM investigations. It can be seen that in all three recovered catalysts most of the particles are glued together forming number of various agglomerates. The particles of recovered carbon and silica supported catalysts seem to be more agglomerated than the particles of CNT-containing catalyst.

Recycling experiments were carried out by recovering the used catalysts samples and reusing them with fresh reagents in

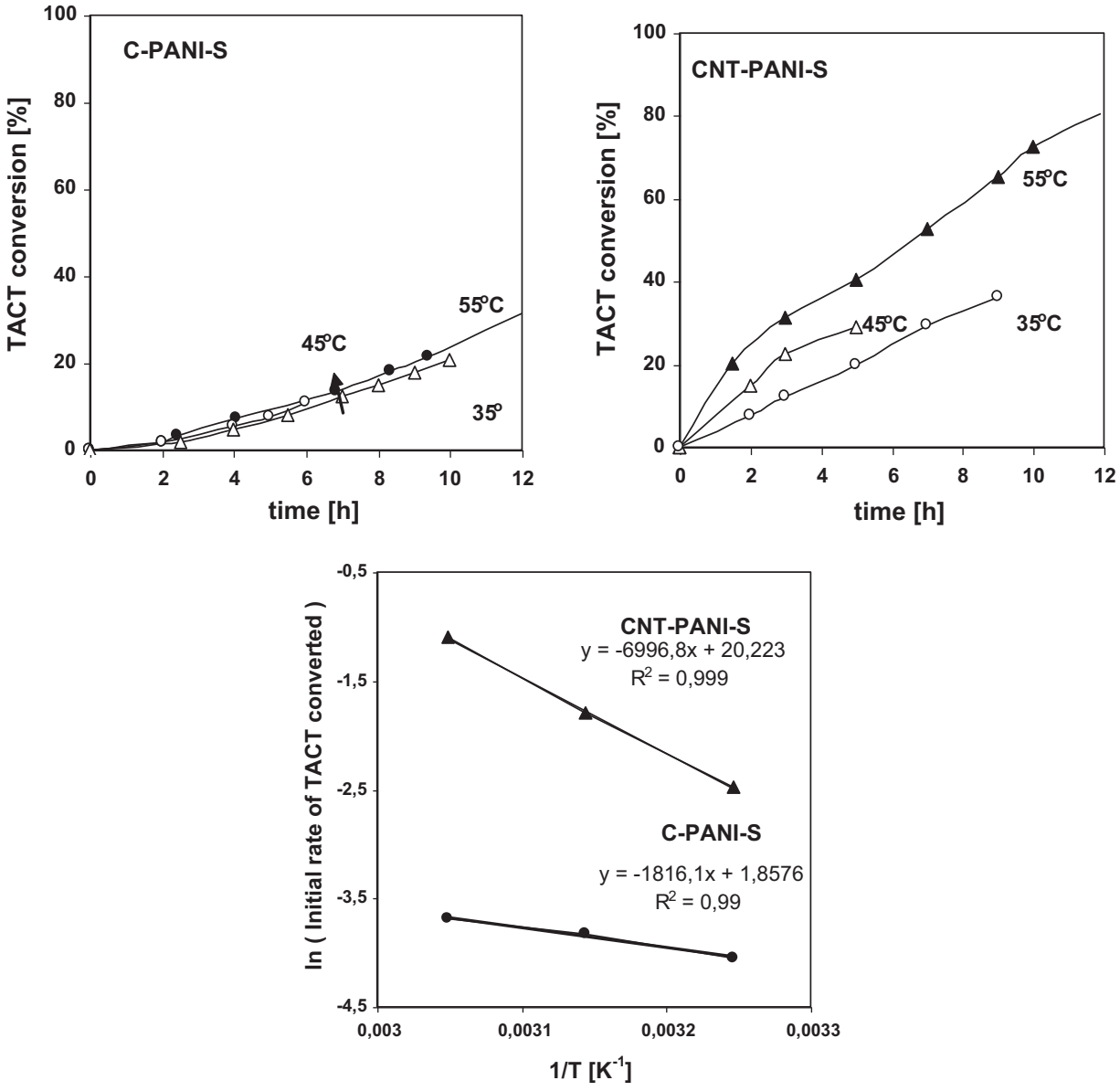

Fig. 11. Methanolysis of triacetin in the presence of CNT-PANI-S and C-PANI-S catalysts. The effect of reaction temperature on the catalyst activity and Arrhenius plot. Reaction conditions: catalyst concentration 15.8 g/dm^3, methanol: TACT = 29:1 molar ratio.

subsequent reaction. The catalysts after first catalytic test were subjected to simple regeneration by washing with methanol/THF mixture followed by drying the samples in contact with air.

The obtained conversion of triacetin (Table 3) shows the activity drop of ca. 10–15%. Similar effect what was observed in our previous work devoted to PANI-S powder catalyst [29]. It was observed that methanolysis of triacetin resulted in slight reduction of acid capacity in the polyaniline sulfate powder and carbon supported PANI-S with low content of polymer (13.6 wt%). After successive reaction cycles using PANI-S powder and this C-PANI-S sample an acid capacities were determined to be 88.6 and 82.2% from the initial ones [19]. However, the activity of fresh and reused catalysts expressed as the rate (mol TACT/min) per active site (mol H^+) was almost stable. For sulfonic acid-based catalysts the reduction of H^+ content during methanolysis of triglycerides and esterification with methanol was also observed by other authors [5,16]. This was ascribed to the possible esterification of the sulfonic acid groups to methyl sulfonates.

Here, the content of acid sites is determined for the samples of recovered catalysts regenerated with methanol/THF mixture. The obtained capacities 1.31, 1.16 and 0.98 mmol H^+/g for C-PANI-S, SiO_2-PANI-S and CNT-PANI-S catalysts respectively, are slightly lower than those in fresh catalysts. As mentioned above, the activity of recovered catalysts drop by ca. 10–15%. As the data in Table 3 show the activity of fresh and reused catalysts expressed as the rate (mol TACT/min) per active site (mol H^+) decreases only slightly. Thus, the observed drop in activity upon recycling experiments could be result of reduction in the content of acid sites, similarly to the observations of other authors and previous effects obtained for PANI-S powder catalyst [19]. These results indicate that organic material including partial glycerides/glycerol appears on the catalysts separated from the reactor. However, simple regeneration of recovered catalysts by the THF/methanol washing procedure restored almost completely their activity.

Let us compare the activity of PANI-S coated catalysts in the methanolysis of vegetable oil, castor oil. As a measure of

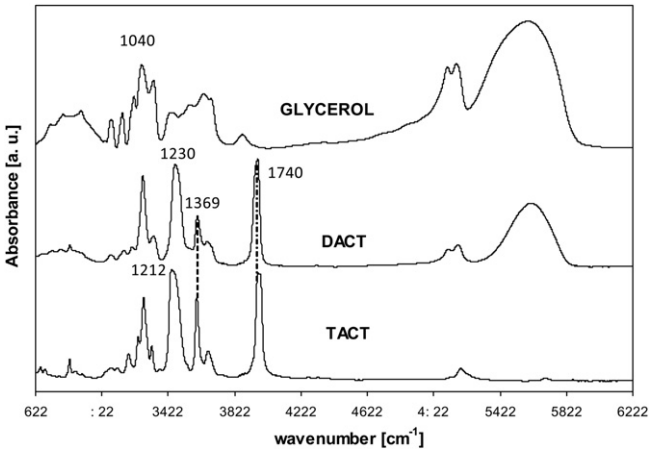

Fig. 12. FT-IR spectra of triacetin, diacetin and glycerol.

catalyst activity initial rate of methyl ester formation (r(ME), mol min^{-1} g^{-1}) was assumed (Table 3). The yield of methyl esters against reaction time is shown in Fig. 14. Similar activity relation can be observed as that in methanolysis of triacetin. The CNT-PANI-S catalyst exhibits the highest activity. The other two C-PANI-S and SiO_2-PANI-S catalysts are definitively less active and their activity does not substantially differ. This latter effect may be explained taking into account that the access of active sites for large triglyceride molecules present in castor oil is more difficult and the observed activity could be mainly related to the centres in outermost surface of the catalysts particles.

The esterification of ricinoleic acid with methanol is studied using CNT-PANI-S and C-PANI-S catalysts. The conversion of ricinoleic acid plotted against the esterification time is displayed in Fig. 15. At the same loading of catalysts (42.9 g/dm^3) the activity of CNT-PANI-S catalyst is ca. 3.5 times higher than that of C-PANI-S sample. This activity relation between CNT and C-supported catalysts in esterification of ricinoleic acid is analogous to that in methanolysis of castor oil. The CNT-PANI-S catalyst is ca. 3.5–4 times more active than other two, silica and carbon-supported samples.

The comparison of activities given in Table 3 demonstrates that the initial activity of all catalysts with polyaniline sulfate coatings in both transesterification reactions is lower than that of PANI-S powder catalyst. However, if the activities related to the proton capacity are taken into consideration, the best performance can be observed for CNT-PANI-S catalyst. This may suggest lower utilization of active sites in all other catalysts and among them in the PANI-S powder sample.

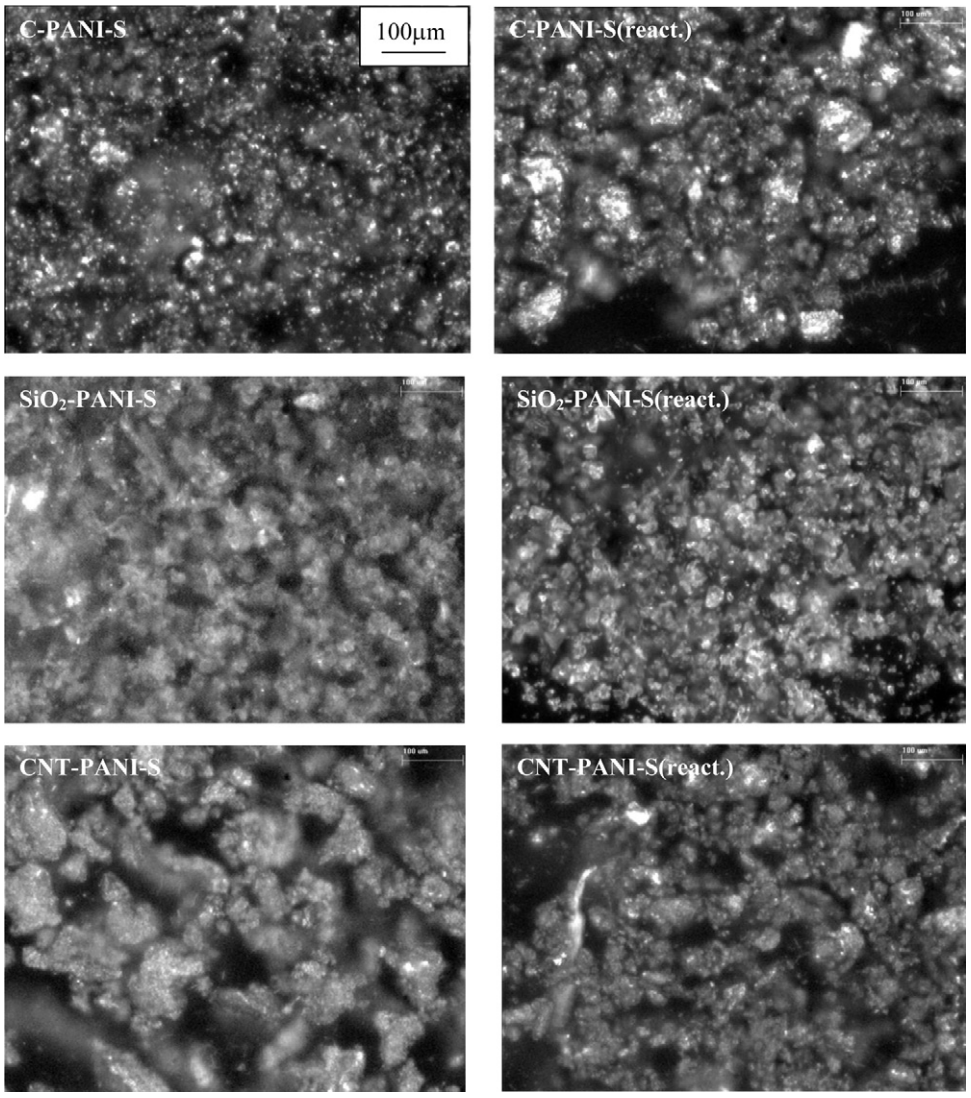

Fig. 13. Images registered by optical microscope for fresh catalysts (left) and the samples recovered after reaction (react.) (right).

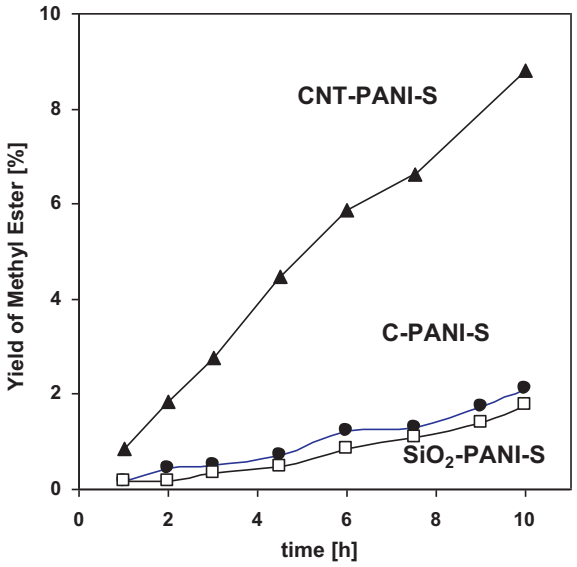

Fig. 14. The yield of methyl esters against reaction time in methanolysis of castor oil in the presence of CNT-PANI-S, C-PANI-S and SiO_2-PANI-S catalysts. Reaction conditions: catalyst concentration 43 g/dm^3, temperature of 55 °C, methanol:triglyceride = 29:1 molar ratio.

The obtained data demonstrate that interaction between partial glycerides/glycerol and active sites occur in all studied catalysts. However, in the C-PANI-S and SiO_2-PANI-S catalysts they result in the effect of "plateau" reaching by partial glycerides and blockage of catalysts. It facilitates the reverse reactions and gives lower conversion of triglycerides. On the other hand, although organic species are also observed on CNT-PANI-S catalyst, their presence does not lead to a blockage of catalyst activity. The CNT material coated with polyaniline sulfate is observed to be the most active catalysts among the studied samples.

As shown in Table 2, the capacity of acid sites and their strength are of similar range in the studied catalysts with polyaniline sulfate coatings. Therefore, the observed difference in the catalysts performance in terms of activity and blockage could be associated with a difference in the morphology of polymer coating and its location throughout the catalysts particles. Porous structure of catalysts could be also considered to be variable determining the observed activity/blockage effects.

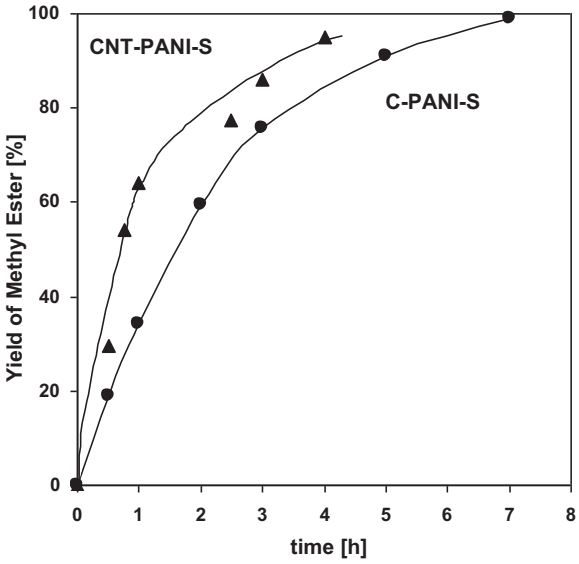

Fig. 15. The yield of methyl ester against reaction time in esterification of ricinoleic acid with methanol in the presence of CNT-PANI-S and C-PANI-S catalysts. Reaction conditions: catalyst concentration 43 g/dm^3, temperature of 60 °C, methanol:ricinoleic acid = 29:1 molar ratio.

As shown in Scheme 1 the protons in –NH^+– groups or in HSO_4^- are located throughout the polymer network. As a result, the access of active sites for the reactants could be determined by the morphology of polymer. However, polymer morphology could also make difficult to some extent the migration of product molecules from the active sites. In both less active C-PANI-S and SiO_2-PANI-S catalysts the coatings of polyaniline sulfate exhibit similar morphology consisting of more or less aggregated fibrous and branched networks. This type of morphology could limit the number of readily accessible acidic sites because of the proton location deeply inside the branched polymer nanorods. As a result, accumulation of more polar products such as glycerol/partial glycerides may be facilitated thus giving a barrier for the reaction. The latter process could be farther facilitated by the microporous structure as in carbon-supported catalyst. On the other hand, although fibrous network of polymer also appears in the silica-containing catalyst blockage of active sites is weaker. This may be associated with lower contribution of microporous structure (Table 1) as well as deposition of polymer mostly onto outer surface of silica particles. It should be pointed out that the blockage of present catalysts manifests very strongly because the protons are located throughout the polyaniline sulfate coating only thus giving high surface density of acid sites. Although this surface location of active sites leads to easy access for the triglycerides molecules it also facilitates a blockage of active sites due to accumulation of more polar reagents. Thus, aggregated and fibrous network of polyaniline sulfate has an adverse influence on catalyst performance in terms of both activity and blockage due to facilitated accumulation of glycerides/glycerol. Maybe, fibrous branched structures of polyaniline sulfate creates a specific spatial organization of the polymer chains resulting in locally increased density of active sites (protons). This facilitates interactions between active sites and polar reagents and in particular with glycerol. On the other hand, a combination of well extended polyaniline sulfate coating together with the mesoporous structure of CNT-PANI-S sample provides conditions for almost uniform surface distribution of active sites. This gives easily accessible active sites for the reactants and almost effectively prevents the accumulation of polar reagents. These features make CNT material coated with polyaniline sulfate an interesting catalyst for methanolysis of triacetin, castor oil as well as for esterification of ricinoleic acid. Hence, the obtained results are consistent with the literature suggestions that catalysts with mesoporous structure are preferred for the transesterification of triglycerides.

4. Conclusions

Polyaniline-sulfate deposited on three different carriers, namely multi-wall carbon nanotubes (CNT), carbon and silica exhibited activity for the transesterification of triacetin and castor oil with methanol. Because of different textural and hydrophobic properties of these carriers, the polymer coatings of various morphologies were obtained. The acid capacity and the strength of acid sites were similar in all studied catalysts.

Uniform coating of CNT with polymer resulted in the most extended polymer coating and the highest activity of the CNT-PANI-S catalyst in all tested reactions. The course of reaction during methanolysis of triacetin on CNT-containing catalyst was similar to that in the presence of soluble sulfuric acid and the maximum yield of methyl esters ca. 95% was attained. The properties of CNT-PANI-S catalyst can be attributed to a combination of mesoporous structure together with well extended polymer coating. This gives easily accessible active sites for the reactants and does not hinder

the migration of reagents from the catalyst. Nanorods of polymer forming branched dendritic structures were formed in carbon and silica carriers. In the presence of these catalysts the accumulation of partial glycerides/glycerol was observed. This was attributed to the aggregated morphology of polymer coating resulting in a locally high density of acid sites. Microporous structure of catalysts as in carbon-supported sample facilitated also this products accumulation effect. Too high density of the active sites, especially inside the pore structure could facilitate interaction with polyol, such as glycerol, which might lead to the accumulation of reagents with consequent blockage of active sites.

Acknowledgement

Studies have been partly supported by the EU Human Capital Operation Program, Polish Project No. POKL.04.0101-00-434/08-00.

References

[1] E. Lotero, Y. Liu, D.E. Lopez, K. Suwannakarn, D.A. Bruce, J.G. Goodwin Jr., Ind. Eng. Chem. Res. 44 (2005) 5353–5363.
[2] M. Zabeti, W.M.A. Daud, M.K. Aroua, Fuel Process. Technol. 90 (2009) 770–777.
[3] M. Di Serio,.R. Tesser, L. Pengmei, E. Santacesaria, Energy Fuels 22 (2008) 207–218.
[4] Z. Helwani, M.R. Othman, A. Aziz, J. Kim, W.J.N. Fernando, Appl. Catal., A 363 (2009) 1–10.
[5] J.A. Melero, J. Iglesias, G. Morales, Green Chem. 11 (2009) 1285–1308.
[6] J. Jitputti, B. Kitiyanan, P. Rangsunvigit, K. Bunyakiat, L. Attanatho, P. Jenvanitpanjakul, Chem. Eng. J. 116 (2006) 61–66.
[7] D.E. Lopez, J.G. Goodwin Jr., D.A. Bruce, E. Lotero, Appl. Catal., A 295 (2005) 97–105.
[8] R.M. de Almedia, L.K. Noda, N.S. Goncalves, S.M.P. Menegethetti, M.R. Meneghetti, Appl. Catal., A 347 (2008) 100–105.
[9] S. Furuta, H. Matsuhashi, K. Arata, Catal. Commun. 5 (2004) 721–723.
[10] S. Furuta, H. Matsuhashi, K. Arata, Biomass Bioenerg. 30 (2006) 870–873.
[11] M.A. Harmer, Q. Sun, Appl. Catal., A 221 (2001) 45–62.
[12] D.E. Lopez, J.G. Goodwin Jr., D.A. Bruce, J. Catal. 245 (2007) 381–391.
[13] B.M.E. Russbueldt, W.F. Hoelderich, Appl. Catal., A 362 (2009) 47–57.
[14] S.M. de Rezende, M. de Castro Reis, M.G. Reid, P.L. da Silva Jr., F.M.B. Coutinho, R.A. da Silva San Gil, E.R. Lachter, Appl. Catal., A 349 (2008) 198–203.
[15] I.K. Mbaraka, K.J. McGuire, B.H. Shanks, Ind. Eng. Chem. Res. 45 (2006) 3022–3028.
[16] J.A. Melero, L.F. Bautista, G. Morales, J. Iglesias, D. Briones, Energy Fuels 23 (2009) 539–547.
[17] L. Sherry, J.A. Sullivan, Catal. Today 175 (2011) 471–476.
[18] A. Zieba, A. Drelinkiewicz, E.N. Konyushenko, J. Stejskal, Appl. Catal., A 383 (2010) 169–181.
[19] A. Zieba, A. Drelinkiewicz, P. Chmielarz, L. Matachowski, J. Stejskal, Appl. Catal., A 387 (2010) 13–25.
[20] S. Palaniappan, M. Sai Ram, Green Chem. 4 (2002) 53–55.
[21] M. Sai Ram, S. Palaniappan, J. Mol. Catal., A 201 (2003) 289–296.
[22] S. Palaniappan, A. John, J. Mol. Catal., A 233 (2005) 9–15.
[23] S. Palaniappan, R.C. Shekhar, Polym. Adv. Technol. 15 (2004) 140–143.
[24] E.T. Kang, K.G. Neoh, K.L. Tan, Prog. Polym. Sci. 23 (1998) 277–324.
[25] A. Malinauskas, Polymer 42 (2001) 3957–3972.
[26] J. Stejskal, I. Sapurina, M. Trchova, Prog. Polym. Sci. 35 (2010) 1420–1481.
[27] J. Stejskal, J. Prokeš, M. Trchová, React. Funct. Polym. 68 (2008) 1355–1361.
[28] J. Stejskal, D. Hlavatá, P. Holler, M. Trchová, J. Prokeš, I. Sapurina, Polym. Int. 53 (2004) 294–300.
[29] A. Riede, M. Helmstedt, I. Sapurina, J. Stejskal, J. Colloid Interface Sci. 248 (2002) 413–418.
[30] I. Sapurina, A. Osadchev, B.Z. Volchek, M. Trchová, A. Riede, J. Stejskal, Synth. Met. 129 (2002) 29–37.
[31] Z. Huang, P.-Ch. Wang, A.G. MacDiarmid, Lamgmuir 13 (1997) 6480–6484.
[32] C.G. Wu, Y.R. Yeh, J.Y. Chen, Y.H. Chiou, Polymer 42 (2001) 2877.
[33] S. Fedorova, J. Stejskal, Langmuir 18 (2002) 5630.
[34] P.-C. Wang, Z. Huang, A.G. MacDiarmid, Synth. Met. 101 (1999) 852–853.
[35] S.S. Pandey, W. Takashima, M. Fuchiwaki, K. Kaneto, Synth. Met. 135–136 (2003) 59–60.
[36] Y. Yang, M. Wan, J. Mater. Chem. 11 (2001) 2022.
[37] E.N. Konyushenko, J. Stejskal, M. Trchova, J. Hradil, J. Kovarova, J. Prokes, M. Cieslar, J.-Y. Hwang, K.-H. Chen, I. Sapurina, Polymer 47 (2006) 5715–5723.
[38] I. Sapurina, M.E. Kompan, A.G. Zabrodski, J. Stejskal, M. Trchova, Russ. J. Electrochem. 43 (2007) 528–536.
[39] J. Stejskal, M. Trchova, S. Fedorova, I. Sapurina, J. Zemek, Langmuir 19 (2003) 3013–3018.
[40] A. Zieba, L. Matachowski, E. Lalik, A. Drelinkiewicz, Catal. Lett. 127 (2009) 183–194.
[41] M.M. Ayad, E.A. Zaki, J. Stejskal, Thin Solid Films 515 (2007) 8381–8385.
[42] I.K. Avlyanov, Synth. Met. 102 (1999) 1272–1273.
[43] M.G. Deng, B.C. Yang, Y.D. Hu, J. Mater. Sci. 40 (5021) (2005), PANI-CNT.
[44] B. Philip, J. Xie, J.K. Abraham, V.K. Varadan, Polym. Bull. 53 (127) (2005), PANI-CNT.
[45] D.G. Cantrell, L.J. Gillie, A.F. Lee, K. Wilson, Appl. Catal. A: Gen. 287 (2005) 183–190.
[46] C.S. MacLeod, A.P. Harvey, A.F. Lee, K. Wilson, Chem. Eng. J. 135 (2008) 63–70.
[47] Y. Pouilloux, S. Abro, C. Vanhove, J. Barrault, J. Mol. Catal. A; 149 (1999) 243–254.
[48] V.K.S. Pappu, A.J. Yanez, L. Peerboom, E. Muller, C.T. Lira, D.J. Miller, Bioresour. Technol. 102 (2011) 4270–4272.
[49] S. Furukawa, Y. Uehara, H. Yamasaki, Bioresour. Technol. 101 (2010) 3325–3332.
[50] X. Liu, X. Piao, Y. Wang, S. Zhu, J. Phys. Chem. A 114 (2010) 3750–3755.
[51] Ch.E.T. Co, M.C. Tan, J.A.R. Diamante, L.R.C. Yan, Catal. Today 174 (2011) 54–58.